AIP Journal of Applied Physics

# Impurity-related optical absorption spectra of GaAs-Ga1−x Al x As cylindrical quantum-well wires

N. Porras-Montenegro, A. Latgé, and Luiz E. Oliveira

Citation: Journal of Applied Physics **70**, 5555 (1991); doi: 10.1063/1.350214

View online: http://dx.doi.org/10.1063/1.350214

View Table of Contents: http://scitation.aip.org/content/aip/journal/jap/70/10?ver=pdfcov

Published by the AIP Publishing

# Impurity-related optical absorption spectra of GaAs-$Ga_{1-x}Al_xAs$ cylindrical quantum-well wires

N. Porras-Montenegro[a] and A. Latgé
*Instituto de Fisica, Universidade Federal Fluminense, Outeiro de São João Batista s/n, Niterói, Rio de Janeiro, 24020, Brazil*

Luiz E. Oliveira
*Instituto de Fisica, Universidade Estadual de Campinas-Unicamp, Caixa Postal 6165, Campinas, São Paulo, 13081, Brazil*

(Received 20 June 1991; accepted for publication 1 August 1991)

The optical-absorption spectra associated with transitions between the $n=1$ valence subband and the donor-impurity band and between the acceptor-impurity band and the $n=1$ conduction subband were calculated for GaAs-$Ga_{1-x}Al_xAs$ cylindrical quantum-well wires of different radii. The distribution of impurities in the wire was assumed to be homogeneous and interaction between the impurities was neglected. The main features in the theoretical spectra were an absorption edge associated with transitions involving impurities at the center of the wire and a peak related to impurities at the edge of the wire. Calculations were performed for both infinite and finite potential barriers, and were compared with previous results in quantum wells of comparable dimensions.

## I. INTRODUCTION

Low-dimensional systems as superlattices and heterostructures have been extensively studied during the last years[1] due to their very particular electronic properties associated with confinement and quantum-size effects. The considerable development of different experimental techniques has made possible the fabrication of ultrathin quantum wells (QW's) and quantum-well wires (QWW's). The latter were first grown from GaAs cladded by $Ga_{1-x}Al_xAs$ with cross-sectional area of the order of 20 nm$\times$20 nm by Petroff *et al.*[2]

In contrast to the one-dimensional electronic confinement in QW's and superlattices, in QWW's the electron is free to move along the axial direction but is confined in its cross-sectional area and quantum size effects become more apparent as this area is reduced. Recently, photoluminescence studies by Tsuchiya *et al.*[3] revealed two intensity peaks associated with electron-light-hole and electron-heavy-hole excitons which constitute the first evidence of two-dimensional quantum confinement. Like in the case of two-dimensional QW's, there is considerable interest in the problem of impurities in QWW's due to their effects on the optical and transport properties of these low-dimensional heterostructures and to their importance on the fabrication of semiconductor devices. Cathodoluminescence experiments[2] in GaAs-$Ga_{1-x}Al_xAs$ QWW's have revealed a small structure in the spectra corresponding to energies red shifted with respect to the exciton line, and with a linewidth of the order of the donor-impurity energy band. Many theoretical studies[4–7] on hydrogenic impurity levels in GaAs-$Ga_{1-x}Al_xAs$ QWW's have shown that the impurity binding energy is higher in QWW's than in QW's due to the additional higher confinement, and goes to infinite when the transversal cross-sectional area decreases if the confining potential is infinite; in a real QWW, however, the confinement potential is finite and the impurity binding energy reaches the limiting value of 1 $R_0^*$ (one effective Rydberg), i.e., the value of the impurity binding energy in the bulk of the cladding material.[5]

Recently, Weber *et al.*[6] have calculated the impurity binding energies and the density of impurity states in rectangular cross-sectional area GaAs-$Ga_{1-x}Al_xAs$ QWW's, finding interesting features in the density of impurity states when the square symmetry of the cross sectional area is lost. Porras-Montenegro *et al.*[8] have calculated the density of impurity states in cylindrical QWW's and found two structures associated to impurities at the center and at the edge of the QWW's, which could, in principle, show up in absorption and photoluminescence spectra associated with shallow hydrogenic impurities in QWW's. They have also studied, for infinite-barrier QWW's, the optical-absorption spectra associated with shallow donor impurities in GaAs-(Ga,Al)As QWW's.

To our knowledge there are no experimental reports on the impurity-related optical and photoluminescence spectra in GaAs-$Ga_{1-x}Al_xAs$ QWW's. Nonetheless, it is certainly of considerable importance a systematic study of the optical-absorption spectra associated with transitions between the valence and donor impurity bands (or between the acceptor and conduction bands) in GaAs-$Ga_{1-x}Al_xAs$ QWW's. This work is organized as follows. In Sec. II we present some of the theoretical aspects concerning the transition probabilities per unit time associated with the impurity-related absorption spectra for both infinite- and finite-barrier GaAs-$Ga_{1-x}Al_xAs$ QWW's. Results and discussion are presented in Sec. III and conclusions in Sec. IV.

[a]Permanent address: Departamento de Fisica, Universidad del Valle, A.A. 24360, Cali, Colombia.

 0021-8979/91/105555-06$03.00  

## II. THEORY

The Hamiltonian of a shallow hydrogenic impurity in a cylindrical QWW of GaAs cladded by $Ga_{1-x}Al_xAs$ can be written in the effective mass approximation as

$$H=\frac{p^2}{2m^*}+\frac{e^2}{\varepsilon_0\,[(\boldsymbol{\rho}-\boldsymbol{\rho}_i)^2+z^2]^{1/2}}+V(\rho), \tag{1}$$

where $m^*$ is the electron effective mass in the band under consideration ($m^*=m_c=0.0665m_0$ for the donor and we have assumed an spherical mass $m^*=m_v=0.30m_0$ for the acceptor; $m_0$ is the free electron mass), $\varepsilon_0$ is the static dielectric constant of the wire material, and $V(\boldsymbol{\rho})$ the confining potential with height depending on the Al concentration on $Ga_{1-x}Al_xAs$. The unitary vector $\hat{\rho}$ defines the direction perpendicular to the wire whereas $\boldsymbol{\rho}_i$ is the impurity position along this direction, and $z$ is the relative separation of the carrier from the impurity along the axial direction of the wire.

For transitions from the first valence subband to a donor impurity level, we have for the initial and final states,[5]

$$\psi^i_{n0k}(\boldsymbol{\rho},z)=\begin{cases}N_1 e^{ikz}J_0(r^v_{10}\rho)u_i(\rho,z) & \rho\leqslant d\\ N_1\dfrac{J_0(r^v_{10}d)}{K_0(b^v_{10}d)}e^{ikz}K_0(b^v_{10}\rho) & u_i(\boldsymbol{\rho},z),\quad \rho\geqslant d\end{cases} \tag{2}$$

$$\psi^f_{n0k}(\boldsymbol{\rho},z)=\begin{cases}N_2 J_0(r^c_{10}\rho)\Gamma(\boldsymbol{\rho},\boldsymbol{\rho}_i,z,\lambda)u_f(\boldsymbol{\rho},z) & \rho\leqslant d\\ N_2\dfrac{J_0(r^c_{10}d)}{K_0(b^c_{10}d)}K_0(b^c_{10}\rho)\Gamma(\boldsymbol{\rho},\boldsymbol{\rho}_i,z,\lambda) & u_f(\boldsymbol{\rho},z)\rho\geqslant d,\end{cases} \tag{3}$$

where $u_i$ and $u_f$ are the periodic parts of the Bloch states for the initial and final states, respectively, $\lambda$ is the variational parameter, $d$ is the wire radius, and,

$$N_1^{-2}=\pi L d^2\left(\frac{K_1(b^v_{10}d)K_{-1}(b^v_{10}d)J_0^2(r^v_{10}d)}{K_0^2(b^v_{10}d)}-J_1(r^v_{10}d)J_{-1}(r^v_{10}d)\right), \tag{4}$$

$$N_2^{-2}=-2\pi\frac{d}{d\lambda}(M_1+M_2), \tag{5}$$

$$M_1=\int_0^d d\rho\,\rho J_0^2(r^c_{10}\rho)I_0(2\lambda\rho_<)K_0(2\lambda\rho_>), \tag{6}$$

$$M_2=\frac{J_0^2(r^c_{10}d)}{K_0^2(b^c_{10}d)}\int_d^\infty d\rho\,\rho K_0^2(b^c_{10}\rho)I_0(2\lambda\rho_<)K_0^2(2\lambda\rho_>), \tag{7}$$

$$\Gamma(\boldsymbol{\rho},\boldsymbol{\rho}_i,z,\lambda)=\exp\{-\lambda[(\boldsymbol{\rho}-\boldsymbol{\rho}_i)^2+z^2]^{1/2}\}, \tag{8}$$

where $L$ is the length of the wire, $J_0$ and $K_0$ are the ordinary and second-kind modified Bessel functions of zero order, respectively, and $r^{c,v}_{10}$ and $b^{c,v}_{10}$ are given by,

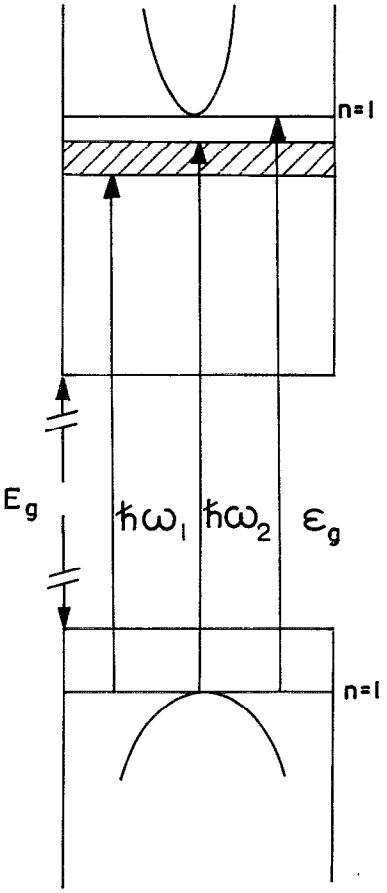


FIG. 1. Schematic representation of some possible absorption transitions in a GaAs-$Ga_{1-x}Al_xAs$ QWW with a donor-impurity band. The parabolas represent a pictorial view of the one-dimensional ($k$ dependence) dispersion of the first conduction—and valence—minibands.

$$r^{c,v}_{10}=\left[\frac{2mE^{c,v}_{10k}}{\hbar^2}-k^2\right]^{1/2};\qquad b^{c,v}_{10}=\left[\frac{2m(V_b-E^{c,v}_{10k})}{\hbar^2}+k^2\right]^{1/2}, \tag{9}$$

with $V_b$ being the constant potential in the barrier material (for the conduction or valence band), $m=m_{c,v}$ and $E^{c,v}_{10k}$ the ground-state corresponding to Eq. (1) without the impurity potential, i.e.,

$$E^{c,v}_{10k}=\frac{\hbar^2}{2m}[(r^{c,v}_{10})^2+k^2]=\frac{\hbar^2}{2m}[k^2-(b^{c,v}_{10})^2]+V_b. \tag{10}$$

Taking the energy origin at the first conduction subband as depicted in Fig. 1, we have for the energy of the initial (first valence subband) state

$$E_i=-\epsilon_g-\frac{\hbar^2k^2}{2m_v}, \tag{11}$$

where $\epsilon_g$ is given by

$$\epsilon_g=E_g+E^c_{10k}+E^v_{10k}, \tag{12}$$

with $E_g$ being the bulk GaAs band gap.

The energy of the final state is

$$E_f = -E_b(d,\rho_i), \tag{13}$$

where $E_b(d,\rho_i)$ is the binding energy of the donor impurity given by

$$E_b(d,\rho_i) = \frac{\hbar^2 (r_{10}^c)^2}{2m_c} - \varepsilon(d,\rho_i), \tag{14}$$

and $\varepsilon(d,\rho_i)$ is the impurity ground-state energy, minimized with respect to $\lambda$.

The transition probability per unit time for valence-to-donor transitions associated with a donor impurity located at $\boldsymbol{\rho}_i$ is proportional to the square of the matrix element of the electron-photon interaction $H_{\text{int}}$ between the wave functions of the initial state (valence) and final (impurity) states, i.e.,

$$W = \frac{2\pi}{\hbar} \sum_i |\langle f|H_{\text{int}}|i\rangle|^2 \delta(E_f - E_i - \hbar w) \tag{15}$$

with $H_{\text{int}} = Ce\cdot\mathbf{p}$, where $\mathbf{e}$ is the polarization vector in the direction of the electric field of the radiation, $\mathbf{p}$ is the momentum operator, and $C$ is a prefactor which contains the photon vector potential.[9] Following the effective mass approximation, the above matrix element may be written as[10,11]

$$\langle f|H_{\text{int}}|i\rangle \cong Ce\cdot\mathbf{p}_{fi} S_{fi}, \tag{16}$$

with

$$\mathbf{p}_{fi} = \frac{1}{\Omega} \int_\Omega d\mathbf{r}\, u_f^*(\mathbf{r}) \mathbf{p} u_i(\mathbf{r}), \tag{17}$$

and

$$S_{fi} = \int d\mathbf{r}\, F_f^*(\mathbf{r}) F_i(\mathbf{r}), \tag{18}$$

where $\Omega$ is the volume of the unit cell and $F_f$ ($F_i$) is the envelope function for the final (initial) state. For the case of the donor impurity we have for $S_{fi} = S_{fi}(\rho_i,\lambda,k(\omega))$,

$$\begin{aligned} S_{fi} = 2N_1N_2 \Bigg[ & \int_0^d \rho d\rho J_0(r_{10}^c\rho) J_0(r_{10}^v\rho) \\ & \times \int_0^\infty dz \cos(kz) \int_0^{2\pi} d\phi\, \Gamma(\boldsymbol{\rho},\boldsymbol{\rho}_i,z,\lambda) \\ & + Q \int_d^\infty \rho d\rho K_0(b_{10}^c\rho) K_0(b_{10}^v\rho) \int_0^\infty dz \cos(kz) \\ & \times \int_0^{2\pi} d\phi\, \Gamma(\boldsymbol{\rho},\boldsymbol{\rho}_i,z,\lambda) \Bigg], \end{aligned} \tag{19}$$

where

$$Q = \frac{J_0(r_{10}^c d)}{K_0(b_{10}^c d)} \frac{J_0(r_{10}^v d)}{K_0(b_{10}^v d)}. \tag{20}$$

For a GaAs-$Ga_{1-x}Al_xAs$ QWW of radius $d$ and length $L$, the transition probability per unit time for valence-to-donor transitions associated with a single impurity located at $\boldsymbol{\rho}_i$ is therefore given by

$$W_d(\rho_i,\omega) = W_0 \left[ \frac{(m_v)^{1/2}\hbar L}{2^{1/2} m_0 a_0^2} \right] \frac{S_{fi}^2(\rho_i,\lambda,(2m_v\Delta/\hbar^2)^{1/2})}{\Delta^{1/2}} \Upsilon(\Delta), \tag{21}$$

where $a_0$ is the Bohr radius and $\Upsilon(\Delta)$ is the step function. In this expression we have

$$\Delta = \hbar\omega - \epsilon_g + E_b(d,\rho_i), \tag{22}$$

and

$$W_0 = \frac{4m_0}{\hbar^3} a_0^2 |C|^2 |\mathbf{e}\cdot\mathbf{p}_{fi}|^2. \tag{23}$$

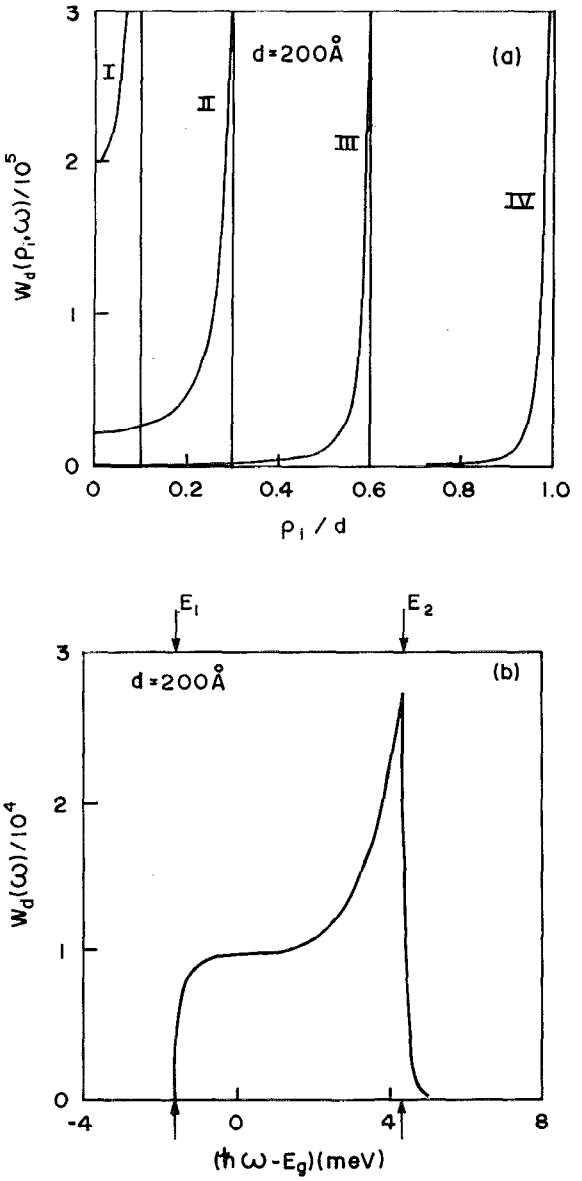


FIG. 2. (a) Absorption probability per unit time $W_d(\rho_i,\omega)$ (in units of $w_0$); for valence-to-donor transitions in a finite GaAs-$Ga_{0.7}Al_{0.3}As$ QWW of radius $d=200$ Å, as a function of the impurity position $\rho_i/d$ and for fixed values of $\hbar\omega - E_g$ given by (i) $-1.57$ meV, (ii) $-1.0$ meV, (iii) 1.0 meV, and (iv) 4.36 meV, respectively. This last value (iv) of $\hbar\omega - E_g$ corresponds to $E_2 = \hbar\omega_2 - E_g$ and signals the onset of transitions to the upper-edge of the donor-impurity band which appears as a peak in the total transition probability per unit time shown in Fig. 2(b).

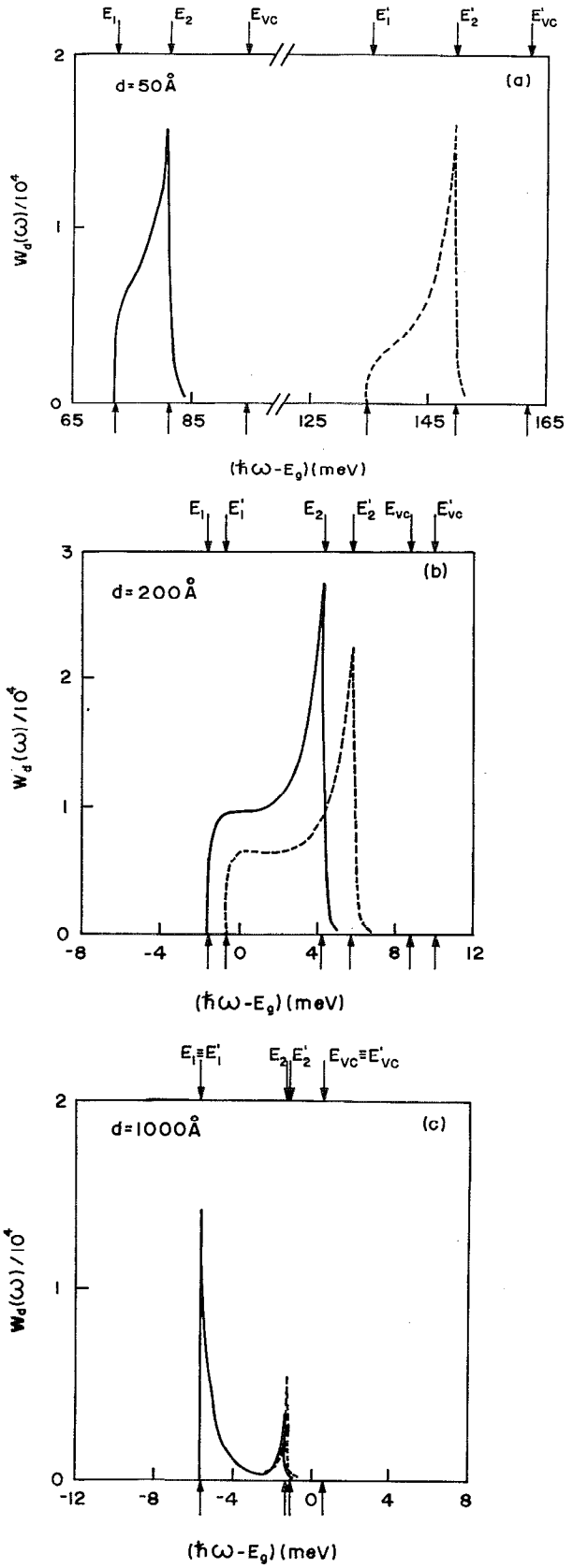


FIG. 3. Optical absorption spectra (in units of $w_0$); for valence-to-donor transitions in finite (full curves) and infinite (dashed curves) GaAs-$Ga_{0.7}Al_{0.3}As$ QWW's of different radii $d=50$ Å (a), 200 Å (b), and 1000 Å (c). $E_1$, $E_2$, and $E_{vc}$ ($E'_1$, $E'_2$, and $E'_{vc}$) correspond, respectively, to the onset of transitions to the donor band, to a peak associated to transitions involving impurities at the edge of the QWW, and to the onset of transitions from the valence to the conduction miniband.

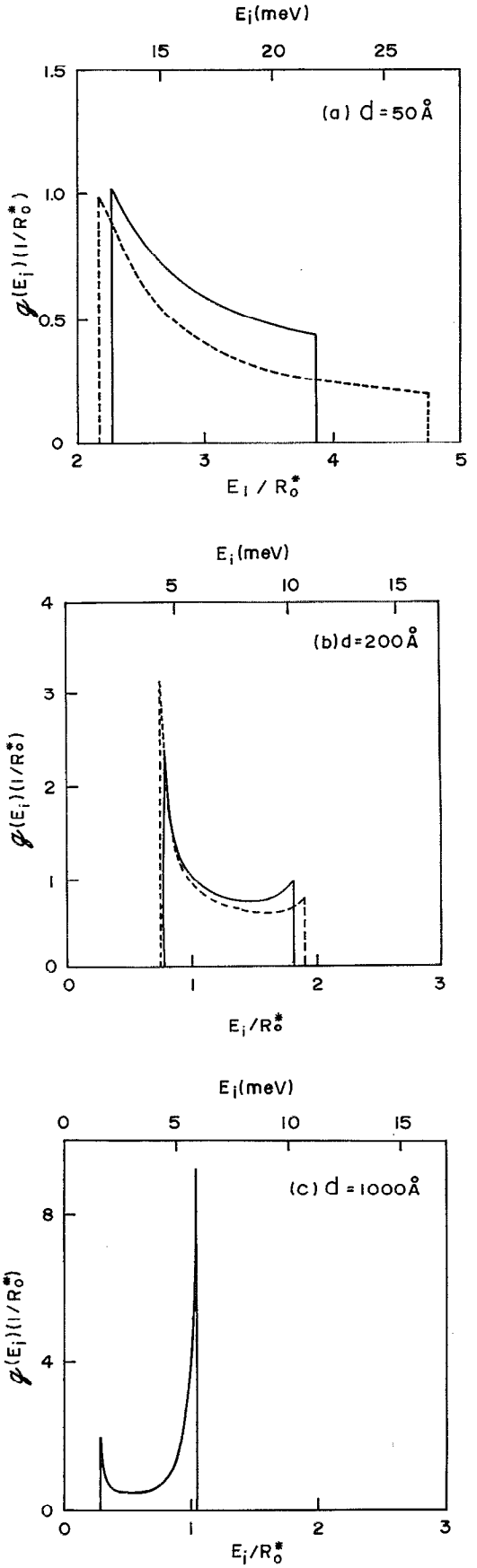


FIG. 4. Density of impurity states for finite (full curves) and infinite (dashed curves) GaAs-$Ga_{0.7}Al_{0.3}As$ QWW's of different radii $d=50$ Å (a), 200 Å (b), and 1000 Å (c).

For a homogeneous distribution of impurities, and assuming that the QWW radius is much larger than the lattice parameter,[12] one has for the total transition probability per unit of time

$$W_d(\omega)=\frac{2}{d^2}\int_0^d d\rho_i\,\rho_i W_d(\rho_i,\omega). \tag{24}$$

The main results of this calculation are presented in the next section. For the case of a finite confining potential, the height of the barrier $V_b$ is taken to be 60% (40%) of the band-gap discontinuity $\Delta E_g(\text{eV})=1.247x$ in the GaAs-$Ga_{1-x}Al_xAs$ QWW for the conduction (valence) band.[13,14] All results are presented for the case of an Al concentration of $x=0.3$ and assuming a homogeneous distribution of impurities inside the GaAs-$Ga_{1-x}Al_xAs$ QWW.

All results above are for the case of a finite-barrier QWW and the corresponding expressions for the infinite-barrier QWW are easily obtained.[5] The case of transitions from an acceptor-impurity band to the first conduction subband is obtained by performing the change $m_v \Rightarrow m_c$ and by exchanging the barrier potencial associated with the valence and conductions subbands.

## III. RESULTS AND DISCUSSION

A schematic representation of a GaAs-$Ga_{1-x}Al_xAs$ QWW doped with a homogeneous distribution of donor impurities is shown in Fig. 1. The edges for optical absorption from the first valence subband to the donor—impurity band is represented by $\hbar\omega_1$ and to the first conduction subband by $\epsilon_g$. The transition $\hbar\omega_2$ corresponds to absorption to an impurity level associated with donors at the edges of the QWW.

Some results of the absorption probability per unit time, $W_d(\rho_i,\omega)$, for valence-to-donor transitions, which is used in Eq. (24) to obtain the total probability function, $W_d(\omega)$, are shown in Fig. 2(a). The absorption $W_d(\rho_i,\omega)$ is given as a function of the impurity position, for some particular values of the photon energy, indicated by $(\hbar\omega - E_g)$, in the case of a finite GaAs-$Ga_{0.7}Al_{0.3}As$ QWW with radius $d=200$ Å; curves I to IV correspond to values of $\hbar\omega - E_g$ equal to $-1.57$, $-1.0$, 1.0, and 4.36 meV, respectively. Curve IV corresponds to the photon energy associated to the peak in the total absorption spectra [cf. Fig. 2(b)]. The energy $E_1=\hbar\omega_1 - E_g$ denotes the absorption threshold; for intermediate $\omega$ values, i.e., for $\omega_1<\omega<\omega_2$, only a fraction of the impurity band contributes to the absorption. Also, notice the divergence of $W_d(\rho_i,\omega)$ when $\rho_i$ approaches a value such that $\hbar\omega=\epsilon_g - E_b(d,\rho_i)$ which may be understood by the divergent behavior of the density of states at the top of the first valence subband. The results in Fig. 2 for a GaAs-(Ga,Al)As QWW should be compared with the corresponding absorption probabilities for a GaAs-(Ga,Al)As QW recently obtained by Oliveira and Pérez-Alvarez.[11]

The absorption spectra for infinite and finite GaAs-$Ga_{0.7}Al_{0.3}As$ QWW's of different radii are shown in Fig. 3. In comparing these results with those of the QW of comparable well width,[11] we observe that the absorption magnitudes are quite similar. A remarkable difference, on the other hand, is the absence of the peak structure associated with impurities located at the center of the well in the QWW, for small radius of the QWW, which is in agreement with the small density of impurity states for impurity positions near the center of the wire as can be seen in Figs. 4(a) and 4(b) for both cases, finite and infinite QWW's. As the wire radius is increased, finite and infinite QWW's begin to exhibit the same absorption spectra appearance since the systems begin to behave as a three-dimensional GaAs. This is clear in Fig. 3(c) where $d=1000$ Å, which can be interpreted as a result close to the bulk limit.[11]

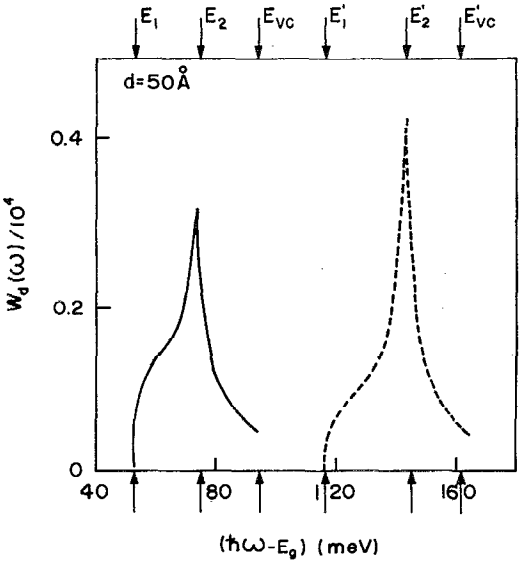


FIG. 5. Optical absorption spectra (in units of $w_0$); for acceptor to conduction-miniband transitions in a finite (full curve) and infinite (dashed curve) GaAs-$Ga_{0.7}Al_{0.3}As$ QWW of radius $d=50$ Å. $E_1$, $E_2$, and $E_{vc}$ ($E_1'$, $E_2'$, and $E_{vc}'$) correspond, respectively, to the onset of transitions from the acceptor band to the conduction miniband, to a peak associated to transitions involving impurities at the edge of the QWW, and to the onset of transitions from the valence to the conduction miniband.

Finally, we present in Fig. 5 the total absorption probability per unit time for transitions of the acceptor-impurity band to the first conduction subband. As it is well known, the case of acceptor-impurities must be treated within the context of a more rigorous treatment due to the coupling of the top four valence bands.[15] Here we have only performed a simplified spherical-effective mass calculation in order to observe the main features of the optical spectra. As in the case of the transitions from the valence to donor-impurity bands, we still have a sharp peak related with transitions involving impurities at the border of the wire in both cases of QWW potential (finite and infinite) and well-defined absorption edges associated with impurities at the center of the wire.

## IV. CONCLUSIONS

We have calculated the optical-absorption spectra associated with transitions between the $n=1$ valence subband and the donor-impurity band for a cylindrical GaAs-

(Ga,Al)As QWW. We have found two structures in the transition probability per unit time, $W_d(\omega)$, i.e., an edge associated with transitions involving impurities at the center of the well and a peak associated with transitions related to impurities at the edge of the well as it has been previously found in QW's. Although experimental results for the optical-absorption spectra associated with impurities in QWW's are not yet available, we believe our results are of importance in the quantitative understanding of future experimental work in this field.

## ACKNOWLEDGMENTS

This work was partially financed by Brazilian Agencies Conselho Nacional de Desenvolvimento Científico e Tecnológico (CNPq), Financiadora de Estudos e Projetos (FINEP) and Fundação de Amparo à Pesquisa do Estado do Rio de Janeiro (FAPERJ).

[1] L. Esaki, in *Recent Topics in Semiconductors Physics*, edited by H. Kamimura and Y. Toyozawa (World-Scientific, Singapore, 1983), p. 1.
[2] P. M. Petroff, A. C. Gossard, R. A. Logan, and W. Wiegmann, Appl. Phys. Lett. **41**, 635 (1982).
[3] M. Tsuchiya, J. M. Gaines, R. H. Yan, R. J. Simes, P. O. Holtz, L. A. Coldren, and P. M. Petroff, Phys. Rev. Lett. **62**, 466 (1989).
[4] G. W. Bryant, Phys. Rev. B **29**, 6632 (1984); Phys. Rev. B **31**, 7812 (1985).
[5] J. W. Brown and H. N. Spector, J. Appl. Phys. **59**, 1179 (1986).
[6] G. Weber, P. A. Schulz, and L. E. Oliveira, Phys. Rev. B **38**, 2179 (1988); G. Weber, P. A. Schulz, and L. E. Oliveira, Mater. Sc. Forum **38–41**, 1415 (1989).
[7] A. Ferreira da Silva, Phys. Rev. B **41**, 1684 (1990).
[8] N. Porras-Montenegro, J. López-Gondar, and L. E. Oliveira, Phys. Rev. B **43**, 1824 (1991); N. Porras-Montenegro and L. E. Oliveira, Solid State Commun. **76**, 275 (1990).
[9] F. Bassani and G. Parravicini, in *Electronic States and Optical Transitions in Solids*, edited by R. A. Ballinger (Pergamon, Oxford, 1975).
[10] R. Perez-Alvarez and P. Pajon-Suarez, Phys. Status Solidi (b) **147**, 547 (1988).
[11] L. E. Oliveira and R. Perez-Alvarez, Solid State Commun. **70**, 523 (1989); Phys. Rev. B **40**, 10460 (1989).
[12] G. Bastard, Phys. Rev. B **24**, 4714 (1981).
[13] R. C. Miller, D. A. Kleinman, and A. C. Gossard, Phys. Rev. B **29**, 7085 (1984).
[14] W. Wang, E. E. Mendez, and F. Stern, Appl. Phys. Lett. **45**, 639 (1984).
[15] W. T. Masselink, Y-C. Chang, and H. Morkoç, Phys. Rev. B **28**, 7373 (1983).